NIH Public Access
Author Manuscript
Gastroenterology. Author manuscript; available in PMC 2011 September 1.

Published in final edited form as:
Gastroenterology. 2010 September ; 139(3): 987–998. doi:10.1053/j.gastro.2010.05.005.

Genetic labeling does not detect epithelial-to-mesenchymal transition (EMT) of cholangiocytes in liver fibrosis in mice

David Scholten[1,2], **Christoph H. Österreicher**[1], **Anjali Scholten**[1], **Keiko Iwaisako**[1], **Guoqiang Gu**[3], **David A. Brenner**[1], and **Tatiana Kisseleva**[1,*]

[1]Department of Medicine, University of California, San Diego, La Jolla, CA 92093, USA

[2]Dept. of Medicine III, University Hospital Aachen, Aachen, Germany

[3]Dept. of Cell and Developmental Biology, Vanderbilt University, Medical Center, Nashville Tennessee, USA

Abstract

BACKGROUND—Chronic injury changes the fate of certain cellular populations, inducing epithelial cells to generate fibroblasts via epithelial-to-mesenchymal-transition (EMT), and mesenchymal cells to generate epithelial cells via mesenchymal-to-epithelial-transition (MET). While the contribution of EMT/MET to embryogenesis, renal fibrosis, and lung fibrosis is well documented, the role of EMT/MET in liver fibrosis is unclear.

AIM—To determine if $K19^+$ cholangiocytes give rise to myofibroblasts (EMT); and/or $GFAP^+$ hepatic stellate cells (HSCs) can express epithelial markers (MET) in response to experimental liver injury.

METHODS—EMT was studied using the Cre-loxP system to map the cell fate of $K19^+$ cholangiocytes in $K19^{YFP}$ or FSP-1^{YFP} mice, generated by crossing of tamoxifen-inducible $K19^{CreERT}$ mice or FSP-1^{Cre} mice with $Rosa26^{f/f\text{-}YFP}$ mice. MET of $GFAP^+$ HSCs was studied in $GFAP^{GFP}$ mice. Mice were subjected to bile duct ligation- (BDL) or CCl_4-liver injury, and livers were analyzed for expression of mesodermal and epithelial markers.

RESULTS—Upon Cre-loxP recombination, > 40% of genetically labeled $K19^+$ cholangiocytes expressed YFP. All mice developed liver fibrosis. However, specific immunostaining of $K19^{YFP}$ cholangiocytes revealed no expression of EMT markers α-SMA, desmin, or FSP-1. Moreover, cells genetically labeled by FSP-1^{YFP} expression did not co-express cholangiocyte markers K19 or E-cadherin. Genetically labeled $GFAP^{GFP}$ HSCs did not express epithelial or liver progenitor markers in response to liver injury.

CONCLUSION—EMT of cholangiocytes identified by genetic labeling does not contribute to hepatic fibrosis in mice. Likewise, $GFAP^{Cre}$ labeled HSCs showed no co-expression of epithelial markers, providing no evidence for MET in HSCs in response to fibrogenic liver injury.

© 2010 The American Gastroenterological Association. Published by Elsevier Inc. All rights reserved.

*Correspondence: tkisseleva@ucsd.edu, Tel:1-858-822-5339.

Publisher's Disclaimer: This is a PDF file of an unedited manuscript that has been accepted for publication. As a service to our customers we are providing this early version of the manuscript. The manuscript will undergo copyediting, typesetting, and review of the resulting proof before it is published in its final citable form. Please note that during the production process errors may be discovered which could affect the content, and all legal disclaimers that apply to the journal pertain.

Disclosures – the authors have no conflict of interest.

Author contribution: D.S., designed the study, and acquired the data, C.O. acquired the data, A.S. performed BDL, G.G provided material support, D.A.B. provided critical revision of the manuscript, T.K. designed the study, wrote the manuscript.

NIH-PA Author Manuscript
NIH-PA Author Manuscript
NIH-PA Author Manuscript

NIH-PA Author Manuscript

NIH-PA Author Manuscript

NIH-PA Author Manuscript

Keywords

Liver fibrosis; EMT; cholangiocytes; MET

INTRODUCTION

Liver cirrhosis, an outcome of chronic liver injury, is characterized by excessive accumulation of extracellular matrix proteins (ECM), mostly type I collagen 1. Hepatic stellate cells (HSCs) are considered to be a major source of ECM 1, but not the only source of myofibroblasts in the injured liver 2. Hepatic myofibroblasts may also originate from portal fibroblasts, interphase (septal) myofibroblasts and, to a smaller extent, bone marrow derived mesenchymal cells 3. Another mechanism, implicated in the fibrogenesis of parenchymal organs is epithelial-to-mesenchymal transition (EMT), when epithelial cells acquire features of mesenchymal cells 4. During this process, epithelial cells detach from the epithelial layer, lose their polarity, expression of epithelial markers (e.g., cytokeratin-19 (K19), CK7, E-cadherin) and tight junction proteins (zonula occludens-1, ZO-1), increase their motility, and obtain a (myo) fibroblastic phenotype 5. Epithelial cells transitioning into (myo)fibroblasts upregulate fibroblast specific protein-1 (FSP-1, a Ca^{2+}-binding S100 protein), which has become a universal marker of EMT during fibrogenesis and cancer [5, 6].

EMT plays an important role in organogenesis during embryonic development [5]. In adult tissues, EMT is a mechanism, which facilitates metastasis and cancer development [7]. In addition, several studies suggest that EMT occurs in response to injury and chronic inflammation, and facilitates fibrosis [5]. EMT in chronic injury has been best characterized in fibrosing kidneys 8. Using gGT-LacZ transgenic mice, which allow identification of tubular epithelial cells in fibrotic kidneys, Iwano et al. demonstrated that more than one third of renal interstitial fibroblasts are derived via EMT 6. Additional studies linked EMT to lung fibrosis, rheumatoid arthritis and retinopathy 8. Meanwhile, the contribution of EMT-derived cells to a population of hepatic myofibroblasts in fibrotic liver is unknown [4]. Typical myofibroblasts, independent of their origin or localization, are identified by the specific morphology (production of the stress fibers), ability to secrete ECM (fibronectin and collagen type I and III), and expression of α-smooth muscle actin (α-SMA) [2]. EMT of hepatocytes has been reported in patients and in mice with liver fibrosis 9. Using genetic fate labeling of $albumin^+$ hepatocytes, Zeisberg et al reported that a population of hepatic FSP-1^+ fibroblasts is derived from mature hepatocytes in response to liver injury [10]. However, only minimal expression of α-SMA was observed in these FSP-1^+ cells (<10%) [10]. In concordance with this data, genetic crossing of albumin-Cre with Rosa-LacZ mice and collagen α1(I)-GFP reporter mice, in which transition of $LacZ^+$ hepatocytes into collagen-expressing myofibroblasts was monitored *in vivo*, detected no EMT-derived myofibroblasts in fibrotic liver [11].

EMT of cholangiocytes has been linked to primary biliary fibrosis (PCB) and NAFLD in patients, rats and mice 12, 13. These studies, specifically in humans, relied mostly on immunohistochemical analysis, and based their conclusions upon the co-localization of epithelial and myofibroblastic markers in the same cells. Generation of cholangiocyte-specific mice (expressing Cre under the control of inducible cytokeratin-19 promoter 14) and EMT-specific mice (expressing Cre under the FSP-1 promoter 15), now makes it possible to trace the fate of cholangiocytes and study their possible EMT in response to injury.

Since EMT reflects inherent cell plasticity, it is closely associated with another process, mesenchymal-to-epithelial transition (MET)4, which is characterized by (trans)differentiation of mesenchymal cells into epithelial cells. It has been suggested that in response to chronic injury, hepatic stellate cells (HSCs) can undergo MET and under certain circumstances acquire

NIH-PA Author Manuscript

NIH-PA Author Manuscript

NIH-PA Author Manuscript

an epithelial phenotype 16. In the course of hepatic fibrosis, HSCs demonstrate unique plasticity by undergoing activation from a quiescent to a myofibroblast phenotype. In their quiescent state, HSCs reside in the space of Disse and store vitamin A 1. They express neural markers, such as glial fibrillary acidic protein (GFAP), synemin and synaptophysin, and mesenchymal/mesodermal markers, such as desmin and vimentin 1. In response to chronic liver injury, quiescent HSCs activate, lose vitamin A droplets and transform into myofibroblasts. Upon activation, HSCs change their morphology, migrate to the site of injury, downregulate neural markers and upregulate mesenchymal markers, e.g. collagen α1(I), α-SMA, and fibronectin. HSC precursors probably originate by embryonic EMT 4. Due to expression of GFAP in quiescent HSCs, MET can be studied in genetically labeled HSCs generated by crossing of $GFAP^{Cre}$ mice with reporter mice. Moreover, new monoclonal antibodies, recognizing a broad variety of hepatic epithelial progenitor cells in mice, provide new reagents to study the mechanism of MET and liver regeneration in fibrotic liver [17].

MATERIALS AND METHODS

Mice

GFAP-Cre mice, ROSA26-$Stop^{f/f\text{-}YFP}$ mice, $Rosa26^{f/f/\text{-}mT/mG}$ mice were obtained from Jackson Laboratories. $K19^{CreERT}$ mice[14] were crossed to homozygosity with $Rosa26^{f/f\text{-}YFP}$ reporter mice and treated with tamoxifen (5 mg/100 μl corn oil × 9 times; Sigma T5648-1G) to achieve Cre-LoxP recombination. $FSP\text{-}1^{Cre}$ mice are a gift of Dr. Nielson. $Col2(I)^{Cre}$ mice are obtained from Dr. Yang. See supplemental materials for details.

Induction of liver injury and measurement of collagen deposition

12 weeks old mice were subjected to bile duct ligation (BDL) or treated with CCl_4 as previously described and hydroxyproline content was measured as described [18]. Liver sections were stained with Sirius red, and positive area was measured in 5 fields/mouse, and quantified using ImageJ.

RT-PCR and real time quantitative PCR

Real-time quantitative RT-PCR was performed using standard conditions using an ABI 7000 sequence detection system (Applied Biosystems), specific primers and SYBRGreen. Ct values of each sample were normalized to 18s mRNA expression. Values were expressed as fold induction in comparison with untreated or sham controls.

Immunofluorescence and immunohistochemistry

Formalin-fixed frozen liver tissues were stained with anti-GFP Ab (Abcam), anti-α-SMA Ab (Abcam), anti-desmin Ab (Thermo Scientific), anti FSP-1 Ab (gift from Dr. Neilson), anti-GFAP Ab (Abcam), anti-pancytokeratin (DakoCytomation), Troma III (DSHB Hibridoma Bank), FITC-conjugated monoclonal anti-α-SMA (Sigma) or the appropriate isotype control, following by secondary Alexa Fluor antibodies and nuclei co-staining with DAPI.. Immunohstochemistry was performed with anti-α-SMA Ab (Abcam) and anti-GFP Ab (Santa Cruz), following by DAB staining (Vector), and counterstaining with Haematoxilin.

HSC isolation and immunostaining

A collagenase-pronase perfusion method was used to isolate HSCs, as previously described [18]. Isolated HSCs were fixed in 4% buffered formalin and stained with anti-GFP Ab and antidesmin antibodies.

NIH-PA Author Manuscript

NIH-PA Author Manuscript

NIH-PA Author Manuscript

Statistics

All data are shown as mean ± SEM. Differences between multiple groups were compared using 1-way ANOVA with post-hoc Bonferroni correction (SPSS 15.0 software). Differences between the 2 groups were compared using a 2-tailed unpaired *t* test (SPSS 15.0 software). *P* values less than 0.05 were considered significant.

RESULTS

Study design

This study was designed to determine if chronic liver injury induces 1) cholangiocytes to contribute to a myofibroblast population via EMT; and 2) HSCs to undergo MET to enforce the regeneration of epithelial cells (hepatocytes and cholangiocytes) and to serve as a facultative source of hepatic progenitors. A genetic approach, based on the Cre-loxP system, was used to label the cells of interest prior to the change of their cellular fate. To study the role of EMT in hepatic fibrosis, cholangiocyte-specific $K19^{CreERT}$ mice [14], in which tamoxifen-inducible CreERT was knocked into the endogenous cytokeratin-19 locus, were crossed with $ROSA26^{f/f\text{-}YFP}$ reporter mice (Fig. 1A). Double transgenic $K19^{YFP}$ offspring, homozygous for Cre and YFP, were treated with tamoxifen (5 mg/mouse, Fig. 1C) to maximally label $K19^{+}$ cholangiocytes with YFP. To identify the cells transitioning into the new phenotype via EMT, $FSP\text{-}1^{Cre}$ mice were crossed with $ROSA26^{f/f\text{-}YFP}$ reporter mice to generate $FSP\text{-}1^{YFP}$ mice, in which the cells expressing FSP-1 are permanently labeled by YFP expression (Fig. 1B). In turn, to study MET, quiescent HSCs were labeled by crossing $GFAP^{Cre}$ mice with $ROSA26^{f/f\text{-}mT/GFP}$ mice (generating $GFAP^{GFP}$ mice), while activated HSCs were labeled by crossing Collagen-α2(I)^{Cre} mice with $ROSA26^{f/f\text{-}YFP}$ mice (generating Col2(I)^{YFP} mice; Fig. 1B).

Induction of liver fibrosis to study EMT in cholangiocytes

To study the role of EMT in hepatic fibrosis, cholangiocyte-specific $K19^{YFP}$ mice were subjected to liver injury by BDL for 21 days or administration of CCl_4 (0.5 μl/g × 16 times) for 2 months (Fig 1C). Similarly, $FSP\text{-}1^{YFP}$ mice, $GFAP^{GFP}$, and Col2(I)^{YFP} mice were subjected to the BDL or CCl_4 using the same treatment protocol.

All mice developed liver fibrosis (Fig. 2A). Hydroxyproline content was increased approximately 3-fold in the livers of BDL-operated $K19^{YFP}$ mice, compared to the sham operated littermates. Sirius red staining reached 9 % in BDL livers versus 1.4 % in sham-operated $K19^{YFP}$ mice. Elevated levels of collagen α1(I) (↑6.8 fold), α-SMA (↑5.3 fold) and FSP-1 protein (↑6 fold) mRNA expression were detected in livers of the BDL- versus sham-operated mice (Fig 2A and B). Similar results were obtained in the CCl_4-treated $K19^{YFP}$ mice, as demonstrated by hydroxyproline content (↑4 times than in control mice), Sirius red staining (↑11 % versus 1.4% in control mice), immunohistochemistry and RT-PCR (Fig. 2A and C). Therefore, we concluded that the liver injury induced by the BDL or CCl_4 resulted in fibrosis so that EMT or MET could be induced in these mice.

Induction of Cre/LoxP recombination in mice to study EMT/MET

Tamoxifen-inducible Cre-loxP recombination was analyzed in $K19^{YFP}$ mice prior to or after liver injury, and compared to untreated mice (no tamoxifen). As expected, only $K19^{YFP}$ mice that received tamoxifen expressed YFP, as detected by specific immunostaining with anti-GFP antibody (Fig. 3A and Suppl. Fig. 1S). Next, the efficiency of Cre-loxP recombination was estimated in control or liver-injured $K19^{YFP}$ mice. As expected, $K19^{YFP}$ cholangiocytes were stained positive with anti-pancytokeratin antibody (Fig. 3A) and localized specifically in the bile ducts, identified by H&E or immunostaining with Troma III antibody (Suppl. Fig. 2S and

NIH-PA Author Manuscript

NIH-PA Author Manuscript

NIH-PA Author Manuscript

3S). The percentage of labeled cholangiocytes was calculated in comparison to the total pancytokeratin (Pan-CK) positive cholangiocytes (100%), and constituted 32 ± 2% in the sham operated $K19^{YFP}$ mice (Fig. 3A and C). Obstruction of the common bile duct causes proliferation of the ductular epithelial cells, and the percentage of YFP-labeled bile ducts increased to 46 ± 7% in BDL $K19^{YFP}$ mice. Similar numbers of YFP^+ cholangiocytes were detected in mice treated with CCl_4 (41 ± 5%) or corn oil (27 ± 6%). The number of genetically labeled cells was quantified in FSP-1^{YFP}, $GFAP^{GFP}$ and Col2(I)^{YFP} mice expressing constitutive Cre, before and after induction of liver injury. The number of YFP^+ cells was significantly increased in the livers of BDL FSP-1^{YFP} mice in comparison with the sham controls (from 31 ± 3% to 3 ± 1%) of total liver cells (100%). Similar results were obtained in CCl_4-treated FSP-1^{YFP} mice (24 ± 2% versus 2 ± 0.6% in control mice), indicating that induction of FSP-1 is a general feature of hepatic fibrosis.

CCl_4 injury also induced activation of HSCs, as indicated by the increased numbers of YFP^+ cells detected in preparations of myofibroblasts (100%) isolated from Col2(I)^{YFP} mice (Fig. 3C). In response to CCl_4 induced injury, the number of genetically labeled HSCs ranged from from 21 ± 4% to 95 ± 3% in Col2(I)^{YFP} mice, and from 82 ± 7% to 84 ± 4% in $GFAP^{GFP}$ mice. Taken together, Cre-loxP recombination was achieved in all transgenic mice and resulted in specific labeling of $K19^+$ cholangiocytes, FSP-1^+ cells, and quiescent $GFAP^+$ and activated Col2(I)$^+$ HSCs. The number of genetically labeled $K19^+$ cholangiocytes, FSP-1^+ cells, and $GFAP^+$ HSCs increased in response to injury (Fig. 3D) in comparison with control mice.

EMT of cholangiocytes does not contribute to the myofibroblast population in fibrotic livers

The role of EMT in the pathogenesis of liver fibrosis was studied in $K19^{YFP}$ mice, in which $K19^+$ cholangiocytes and their progeny were permanently labeled by YFP expression. In addition to existing cholangiocytes, repeated tamoxifen administration induced expression of YFP in new cholangiocytes in response to injury. YFP^+ cholangiocytes were located in the portal areas (Fig. 4A). EMT in the YFP^+ cholangiocytes was evaluated in $K19^{YFP}$ mice with liver fibrosis, and was determined by co-expression of mesenchymal markers (α-SMA, desmin) in cells with a history of K19 expression. Expression of GFAP, a marker of HSCs, was not detected in YFP^+ cholangiocytes. Immunostaining with anti-α-SMA and anti-desmin antibodies, which detect myofibroblasts, revealed no co-localization of α-SMA or desmin in YFP^+ cells in livers of BDL-operated $K19^{YFP}$ mice. Similarly, double positive YFP^+ α-SMA^+ or $YFP^+desmin^+$ cells were not observed in CCl_4-treated $K19^{YFP}$ mice, suggesting that EMT of cholangiocytes does not produce myofibroblasts in response to experimental liver fibrosis. To corroborate these results, the myofibroblast population was purified using gradient centrifugation method from fibrotic livers of BDL-injured $K19^{YFP}$ or Col2(I)^{YFP} mice. No YFP positive cells were detected in these cultures from $K19^{YFP}$ mice, while in control experiments 97 ± 3% of myofibroblasts, derived from Col2(I)^{YFP} mice, expressed YFP. Thus, our results demonstrate that EMT of genetically labeled cholangiocytes does not contribute to HSCs, or myofibroblasts, as demonstrated using two models of experimental hepatic fibrosis.

Cholangiocytes do not upregulate FSP-1 in response to fibrogenic liver injury

We hypothesized that cholangiocytes may undergo an incomplete EMT, and, therefore, would express FSP-1, without being transformed into myofibroblasts. Livers from BDL- or CCl_4-injured $K19^{YFP}$ mice were analyzed for the EMT marker FSP-1 expression. Although FSP-1^+ and $K19^{YFP+}$ cells were located in the portal areas in a close proximity to each other, there was no co-localization (Fig. 4C, panel a).

We next examined expression of FSP-1 on epithelial cells. We used FSP-1-GFP reporter mice, which express GFP under control of the FSP-1 promoter and mark cells currently expressing FSP-1 [6]. FSP-1-GFP mice were subjected to BDL, and the livers were stained with anti-

NIH-PA Author Manuscript

NIH-PA Author Manuscript

NIH-PA Author Manuscript

pancytokeratin (Pan-CK) antibody to visualize cholangiocytes. Pan-CK positive cholangiocytes were located in the portal areas of FSP-1-GFP mice, but never overlapped with FSP-1-GFP$^+$ cells, indicating that cholangiocytes did not express FSP-1 (Fig. 4C, panel b). Similar results were obtained for CCl_4 treated mice. Since expression of FSP-1$^+$ by cells of epithelial origin may be transient during EMT, we next examined the fate of FSP-1 expressing cells. To address this question, FSP-1^{YFP} mice, generated by crossing FSP-1^{Cre} mice with Rosa26$^{f/f\text{-}YFP}$ mice, were used to identify the progeny of FSP-1$^+$ cells, even if these cells completed EMT and downregulated FSP-1 expression. Liver from BDL- or CCl_4- treated FSP-1^{YFP} mice were co-stained with anti-GFP and anti-Pan-CK antibodies (Fig. 4C, panel c). Examination of YFP$^+$ cells revealed no co-expression of Pan-CK, suggesting that cholangiocytes did not express FSP-1 before or during liver injury. Consistent with this, cholangiocytes immunostained with anti-Pan-CK$^+$ antibody did not express α-SMA in response to BDL or CCl_4 (Suppl. Fig. 4S).

EMT is best characterized during embryonic development, and usually occurs between day E6.5 (gastrulation) and day E9.5 [19]. Since K19 is strongly upregulated in tissues during gastrulation (> 90% cells) 14, Cre-loxP recombination was induced in embryos at day E9.5 by tamoxifen administration to pregnant K19^{YFP} mice. Embryos (labeled at E9.5) contained K19-YFP$^+$ cells. The majority of YFP$^+$ cells were located in the skin, epithelial lining, lungs and liver (Suppl. Fig. 5S). FSP-1$^+$ cells co-localized with K19-YFP$^+$ cells, mainly in the lungs, indicating that K19-expressing cells undergo EMT during embryogenesis. Furthermore, immunostaining with anti-α-SMA or anti-desmin antibodies also identified double positive cells. In particular, desmin$^+$ K19^{YFP+} cells were identified in the developing gastrointestinal tract. Hence, K19^{YFP} mice are well suitable to study EMT during embryogenesis.

Cell fate mapping of hepatic stellate cells to study MET in liver fibrosis

MET is a process opposite to EMT, in which myofibroblasts undergo differentiation into epithelial-like cells [4]. To follow the fate of hepatic stellate cells in adult mice in response to liver fibrosis, GFAP^{Cre} mice were crossed with Rosa26$^{f/f\text{-}mT/GFP}$ mice to generate GFAP^{GFP} mice (Fig. 5A and 3C). These mice demonstrated successful Cre-loxP recombination by expression of GFP in the GFAP$^+$ cells, but not in Tomato-red$^+$ hepatocytes. To induce liver injury, GFAP^{GFP} mice were treated with CCl_4, and the ability of HSCs to undergo MET in response to acute injury or during recovery was assessed by immunostaining with anti-α-SMA, anti-desmin, anti-Pan-CK and E-cadherin antibodies. As expected, activated HSCs proliferated, migrated into fibrotic septa and expressed myofibroblastic markers α-SMA and desmin (Fig. 5B). Double positive α-SMA$^+$GFP$^+$ and desmin$^+$GFP$^+$ cells were visualized by pseudo-red cytosolic staining surrounded by membrane tagged GFP signal. Although the epithelial marker E-cadherin was detected in fibrotic areas of GFAP^{GFP} livers, it did not co-localize with the GFAP^{GFP+} HSCs (Fig. 5B). Similar results were obtained for Pan-CK$^+$ cholangiocytes, although located in close proximity to HSCs, revealed no co-localization with GFAP^{GFP+} cells (Fig. B and C).

As an alternative approach to assess MET, Collagen α2(I)-Cre mice were crossed with Rosa26$^{f/f\text{-}YFP}$ mice, and collagen-expressing activated HSCs (as well as any other myofibroblasts) were analyzed for expression of MET markers in response to CCl_4-induced liver injury (Fig. 5D). However, similarly to GFAP^{GFP} mice, Col^{YFP+} cells showed no co-localization with Pan-CK$^+$ cholangiocytes.

To further analyze the concept of stellate cell plasticity, livers from CCl_4-treated GFAP^{GFP} mice were stained for markers specific for murine oval cells [17]. Several antibodies have recently been generated that recognize progenitors in DDC-induced mice. Although these antibodies recognized a small number of progenitors in CCl_4-treated mice, we did not find any GFAP^{GFP+} labeled HSCs staining for these markers (Fig. 6).

NIH-PA Author Manuscript

NIH-PA Author Manuscript

NIH-PA Author Manuscript

DISCUSSION

Chronic inflammation and persistent liver injury may induce deregulation of normal physiology with inherent cellular plasticity, causing EMT and/or MET. Although both processes may enhance regeneration, they may also accelerate the progression of liver fibrosis. Using two models of liver fibrosis, BDL and CCl_4, we have determined that genetically labeled $K19^+$ cholangiocytes do not undergo EMT. While FSP-1^+ cells were widely present in fibrotic livers, this marker was not upregulated in Pan-CK^+ cholangiocytes. Moreover, fibrogenic liver injury did not prompt hepatic stellate cells to express epithelial cell markers, such as pancytokeratin or E-cadherin. HSCs also lacked markers of hepatic progenitors. Taken together, the current study provides evidence that EMT in cholangiocytes and MET in HSCs does not contribute to experimental hepatic fibrosis or liver regeneration.

Recent studies have reported that EMT plays a role in biliary fibrosis in humans, rats and mice [12]. Using mostly immunohistochemical analysis, EMT in cholangiocytes was identified by co-localization of the EMT-specific marker FSP-1 in CK-7^+ cells [12, 13 20]. Although these studies demonstrated co-staining in CK-7^+ cells, the contribution of EMT to the deposition of extracellular matrix and fibrosis was not documented. Moreover, EMT was solely based on co-expression of FSP-1 and CK-7, or examination of EMT-activated signal transduction pathways in response to injury [9], without following cholangiocyte differentiation into cells with mesenchymal phenotype. Taken together, detection of EMT in humans and rodents provides several difficulties: 1) specificity of antibodies used for immunohistochemistry, such as CK-7, may recognize a population slightly distinct from $K19^+$ or Pan-CK^+ cholangiocytes; 2) Co-expression of FSP-1 and epithelial markers (CK-7, Pan-CK or K19), typical for early EMT, may be transient. Therefore, finding no co-expression of these markers does not rule out the occurrence of EMT; 3) Co-localization studies may generate false positives by bleed-through of fluorescent probes or by overlapping cells expressing different markers being misinterpreted as single cells. To overcome these obstacles, genetic *in vivo* labeling of the cells of interest, $K19^+$ cholangiocytes, and monitoring their changing phenotype throughout duration of the liver injury, was considered as the method of choice in the current study.

We genetically labeled $K19^+$ cholangiocytes in adult mice to investigate EMT in response to fibrogenic liver injury. Tamoxifen-inducible $K19^{CreERT}$ mice were chosen for a number of reasons: 1) To avoid genetic labeling of $K19^+$ cells occurring during embryonic development, the tamoxifen-inducible Cre-ERT gene was knocked into the genetic locus of the K19 promoter [14]; 2) The K19 promoter is highly specific for cholangiocytes in the liver, as confirmed by immunostaining with anti-K19 and Pan-CK antibodies; 3) Upregulation of mesenchymal markers (FSP-1, α-SMA and desmin) is monitored in K19-labeled cholangiocytes throughout liver injury, tracing initial (epithelial) and final (mesenchymal) phenotypes in a single cells; 4) BDL causes maximal damage to the biliary epithelium with proliferation of the bile ducts, a condition which has been proposed to induce EMT. Thus, using $K19^{YFP}$ mice ($K19^{CreERT}$ mice × $Rosa26^{f/f\text{-}YFP}$ mice), we have shown that cells with a history of K19 expression did not express α-SMA or desmin, mesenchymal markers typically expressed by myofibroblasts. Furthermore, K19-labeled cholangiocytes did not co-express FSP-1, a marker associated with EMT, suggesting that fibrogenic liver injury does not induce EMT in cholangiocytes.

Our results differ from the findings reported by Omenetti et al [12] and Roderfeld et al [20], who demonstrated co-expression of FSP-1 in CK-7 positive biliary cells. Several factors may explain this discrepancy. First, inducible $K19^{Cre}$ mice label a highly specific population of mature cholangiocytes at the time of injury. And, unlike previously reported CK-7^+ cells, this $K19^+$ cholangiocyte subset may not be involved in EMT. In concordance with this assumption, a population of $K19^+/CK7^-$ cholangiocytes was identified in adult rats. These $K19^+/CK7^-$ cholangiocytes proliferated after 2-acetaminofluorene (AAF) administration and were located

NIH-PA Author Manuscript

NIH-PA Author Manuscript

NIH-PA Author Manuscript

in the smaller branches of the biliary tree including the canals of Hering [21]. Second, although we have demonstrated that $K19^+$ cholangiocytes proliferate in response to BDL-liver injury, the population of cholangiocytes is heterogenous. This fact is supported not only by identification of $K19^+/CK\text{-}7^-$ cholangiocytes, but also by presence of oval cells and other liver progenitors in the canal of Hering [17]. Third, development of liver fibrosis often depends on the model of injury and the choice of transgenic/knockout mice. Thus, for example, Omenetti at al. studied Ptc-deficient mice, while Roderfeld et al used $Abcb4^{-/-}$ mice. Our current study focused on EMT in $K19^+$ cholangiocytes in wild type mice undergoing experimental fibrosis. To strengthen our findings, we analyzed cells that might have undergone EMT and at some point upregulated FSP-1 in response to injury. However, genetically labeled FSP-1^+ cells did not express cholangiocyte markers (Pan-CK), proving that cholangiocytes did not express FSP-1 and do not undergo EMT in response to experimental liver fibrosis. Of course, all of these genetic mouse experiments are limited by the short duration of the studies (usually 2–8 weeks) in comparison to the years in which liver fibrosis progresses in patients. Therefore EMT of cholangiocytes in patients, originally defined by co-expression of epithelial and myofibroblasts-like markers [22–24], cannot be excluded.

Unfortunately, the genetic studies of EMT in fibrosis using Cre-LoxP system has its own limitations. Genetic labeling of a specific cellular population is achieved by crossing mice expressing Cre under control of a cell-specific promoter with reporter mice, ubiquitously expressing the β-*gal* or *yfp* genes in which transcription is blocked by a *floxed* Stop cassette [25]. The choice of the reporter mice is critically significant, and $Rosa26^{f/f\text{-}YFP}$ mice are superior to $Rosa26^{f/f\text{-}\beta\text{-}gal}$ mice, which increase non-specific β-gal accumulation in tissues with age. Two problems are associated with cell fate mapping in mice: specificity of Cre and efficiency of Cre-lox recombination. Since specificity of Cre expression can be confirmed by immunostaining, efficiency of Cre-lox recombination is solely dependent on Cre concentration. Therefore, 100% of Cre-lox recombination can be rarely achieved in mice. It is especially difficult in ER-Cre mice, in which Cre expression is regulated by tamoxifen administration and can be strongly affected by the dose, route, frequency of administration [26]. A number of well established Cre- or ER-Cre mice have incomplete Cre-Lox recombination, which creates problems with conditional gene ablation in mice [27]. However, the Cre-lox-system remains the most reliable tool to monitor specific cellular populations and their progeny in mice. Thus, using Albumin-Cre mice complete Cre-LoxP recombination was not achieved in hepatocytes, but still demonstrated the lack of EMT in response to injury [11]. Low efficiency of Cre-LoxP recombination can be overcome in cell fate mapping studies by examining a large number of mice per experiment and cells per mouse. This way a statistically significant result can be obtained. Since we were not able to determine any genetically labeled cells co-expressing markers of EMT in more than 1000 $K19^{YFP+}$ cells, (e.g. α-SMA and $K19^{YFP}$, or desmin and $K19^{YFP}$), this number was not increased when calculated for 100% of cholangiocytes.

Our present study also investigated the role of MET of hepatic stellate cells (HSCs) in response to liver injury. Again, using a genetic approach, we showed that neither quiescent $GFAP^+$-labeled nor activated collagen-$\alpha2(I)^+$-labeled HSCs express epithelial cell or cholangiocyte markers following CCl_4-activation or recovery. Our findings differ from Yang et al, who suggested that quiescent HSCs may differentiate into hepatocytes, and, therefore, belong to the oval cell family [28]. Due to the expression of neural markers, HSCs are believed to originate during embryonic development from the same common precursor as brain astrocytes. In addition, it has been suggested that adult bone marrow can serve as a source of HSC replenishment in response to injury [29]. Recent studies in rats suggested that, in addition to epithelial cells, Thy-1.1^+ oval cells may also give rise to cells with myofibroblastic phenotype [30]. Moreover, expression of progenitor markers CD133 raised a possibility that HSCs may arise from a common liver precursor (or liver stem cell) in the adult liver [28]. Using

NIH-PA Author Manuscript

NIH-PA Author Manuscript

NIH-PA Author Manuscript

immunostaining with recently generated monoclonal antibodies for the oval cell response in ductal and periductal areas 17, we demonstrated that GFP-labeled HSCs from CCl_4-treated $GFAP^{GFP}$ mice lack markers of oval cells. Although our study does not provide insight into whether there is a common hepatic precursor cell for HSCs, hepatocytes, and cholangiocytes, it does demonstrate that HSCs and myofibroblasts did not undergo MET to become epithelial cells.

Supplementary Material

Refer to Web version on PubMed Central for supplementary material.

Acknowledgments

Grant Support: - 2 P50 AA011999-11 NIH/NIAAA; Liver scholar Research Award, ALF. Dr. David Scholten was funded by the Rotation program of the Medical Faculty, RWTH Aachen.

Abbreviations

EMT	Epithelial-to-mesenchymal transition
MET	cholangiocytes, liver fibrosis, mesenchymal-to-epithelial transition
HSCs	queiscent and activated hepatic stellate cells
CreERT	tamoxifen-inducible Cre
ECM	extracellular matrix
$Rosa26^{f/f\text{-}YFP}$ mice	Rosa26-flox-Stop-flox-EYFP reporter mice
$Rosa26^{f/f\text{-}mT/mGFP}$	Rosa26-flox-Tomato-$Red^{membrane\text{-}tagged}$-Stop-flox-$GFP^{membrane\text{-}tagged}$
K19	cytokeratin-19 (cholangiocyte marker)
Pan-CK	pancytokeratin (cholangiocyte marker)
FSP-1	fibroblast specific protein-1 (EMT marker)
α-SMA	α-smooth muscle actin (myofibroblast marker)
GFAP	glial fibrillary acidic protein
Col2(I)	collagen α2(I)

REFERENCES

1. Bataller R, Brenner DA. Liver fibrosis. J Clin Invest 2005;115:209–218. [PubMed: 15690074]
2. Parola M, Marra F, Pinzani M. Myofibroblast - like cells and liver fibrogenesis: Emerging concepts in a rapidly moving scenario. Mol Aspects Med 2008;29:58–66. [PubMed: 18022682]
3. Kisseleva T, Brenner DA. Fibrogenesis of parenchymal organs. Proc Am Thorac Soc 2008;5:338–342. [PubMed: 18403330]
4. Choi SS, Diehl AM. Epithelial-to-mesenchymal transitions in the liver. Hepatology. 2009
5. Zeisberg M, Neilson EG. Biomarkers for epithelial-mesenchymal transitions. J Clin Invest 2009;119:1429–1437. [PubMed: 19487819]
6. Iwano M, Plieth D, Danoff TM, Xue C, Okada H, Neilson EG. Evidence that fibroblasts derive from epithelium during tissue fibrosis. J Clin Invest 2002;110:341–350. [PubMed: 12163453]
7. Huber MA, Kraut N, Beug H. Molecular requirements for epithelial-mesenchymal transition during tumor progression. Curr Opin Cell Biol 2005;17:548–558. [PubMed: 16098727]

NIH-PA Author Manuscript

NIH-PA Author Manuscript

NIH-PA Author Manuscript

8. Kalluri R, Weinberg RA. The basics of epithelial-mesenchymal transition. J Clin Invest 2009;119:1420–1428. [PubMed: 19487818]
9. Nitta T, Kim JS, Mohuczy D, Behrns KE. Murine cirrhosis induces hepatocyte epithelial mesenchymal transition and alterations in survival signaling pathways. Hepatology 2008;48:909–919. [PubMed: 18712785]
10. Zeisberg M, Yang C, Martino M, Duncan MB, Rieder F, Tanjore H, Kalluri R. Fibroblasts derive from hepatocytes in liver fibrosis via epithelial to mesenchymal transition. J Biol Chem 2007;282:23337–23347. [PubMed: 17562716]
11. Taura, K.; Miura, K.; Iwaisako, K.; Österreicher, CH.; Kodama, Y.; Penz-Österreicher, M.; Brenner, DA. Hepatocytes do not undergo epithelial-mesenchymal transition in liver fibrosis in mice. Vol. Volume 9999. NA: 2009.
12. Omenetti A, Porrello A, Jung Y, Yang L, Popov Y, Choi SS, Witek RP, Alpini G, Venter J, Vandongen HM, Syn WK, Baroni GS, Benedetti A, Schuppan D, Diehl AM. Hedgehog signaling regulates epithelial-mesenchymal transition during biliary fibrosis in rodents and humans. J Clin Invest 2008;118:3331–3342. [PubMed: 18802480]
13. Syn WK, Jung Y, Omenetti A, Abdelmalek M, Guy CD, Yang L, Wang J, Witek RP, Fearing CM, Pereira TA, Teaberry V, Choi SS, Conde-Vancells J, Karaca G, Diehl AM. Hedgehog-Mediated Epithelial-to-Mesenchymal Transition and Fibrogenic Repair in Nonalcoholic Fatty Liver Disease. Gastroenterology. 2009
14. Means AL, Xu Y, Zhao A, Ray KC, Gu G. A CK19(CreERT) knockin mouse line allows for conditional DNA recombination in epithelial cells in multiple endodermal organs. Genesis 2008;46:318–323. [PubMed: 18543299]
15. Bhowmick DA, Zhuang Z, Wait SD, Weil RJ. A functional polymorphism in the EGF gene is found with increased frequency in glioblastoma multiforme patients and is associated with more aggressive disease. Cancer Res 2004;64:1220–1223. [PubMed: 14973082]
16. Kuo TK, Hung SP, Chuang CH, Chen CT, Shih YR, Fang SC, Yang VW, Lee OK. Stem cell therapy for liver disease: parameters governing the success of using bone marrow mesenchymal stem cells. Gastroenterology 2008;134:2111–2121. 2121 e1–3. [PubMed: 18455168]
17. Dorrell C, Erker L, Lanxon-Cookson KM, Abraham SL, Victoroff T, Ro S, Canaday PS, Streeter PR, Grompe M. Surface markers for the murine oval cell response. Hepatology 2008;48:1282–1291. [PubMed: 18726953]
18. Seki E, de Minicis S, Inokuchi S, Taura K, Miyai K, van Rooijen N, Schwabe RF, Brenner DA. CCR2 promotes hepatic fibrosis in mice. Hepatology 2009;50:185–197. [PubMed: 19441102]
19. Nakaya Y, Sheng G. Epithelial to mesenchymal transition during gastrulation: an embryological view. Dev Growth Differ 2008;50:755–766. [PubMed: 19046163]
20. Roderfeld M, Rath T, Voswinckel R, Dierkes C, Dietrich H, Zahner D, Graf J, Roeb E. Bone marrow transplantation demonstrates medullar origin of CD34(+) fibrocytes and ameliorates hepatic fibrosis in Abcb4(−/−) mice. Hepatology. 2009
21. Paku S, Dezso K, Kopper L, Nagy P. Immunohistochemical analysis of cytokeratin 7 expression in resting and proliferating biliary structures of rat liver. Hepatology 2005;42:863–870. [PubMed: 16175606]
22. Xia JL, Dai C, Michalopoulos GK, Liu Y. Hepatocyte growth factor attenuates liver fibrosis induced by bile duct ligation. Am J Pathol 2006;168:1500–1512. [PubMed: 16651617]
23. Rygiel KA, Robertson H, Marshall HL, Pekalski M, Zhao L, Booth TA, Jones DE, Burt AD, Kirby JA. Epithelial-mesenchymal transition contributes to portal tract fibrogenesis during human chronic liver disease. Lab Invest 2008;88:112–123. [PubMed: 18059363]
24. Diaz R, Kim JW, Hui JJ, Li Z, Swain GP, Fong KS, Csiszar K, Russo PA, Rand EB, Furth EE, Wells RG. Evidence for the epithelial to mesenchymal transition in biliary atresia fibrosis. Hum Pathol 2008;39:102–115. [PubMed: 17900655]
25. Austin S, Sternberg N, Yarmolinsky M. Miniplasmids of bacteriophage P1. I. Stringent plasmid replication does not require elements that regulate the lytic cycle. J Mol Biol 1978;120:297–309. [PubMed: 642010]
26. Feil R. Conditional somatic mutagenesis in the mouse using site-specific recombinases. Handb Exp Pharmacol 2007:3–28. [PubMed: 17203649]

NIH-PA Author Manuscript

NIH-PA Author Manuscript

NIH-PA Author Manuscript

27. Birling MC, Gofflot F, Warot X. Site-specific recombinases for manipulation of the mouse genome. Methods Mol Biol 2009;561:245–263. [PubMed: 19504076]

28. Yang L, Jung Y, Omenetti A, Witek RP, Choi S, Vandongen HM, Huang J, Alpini GD, Mae Elizabeth Diehl A. Fate-Mapping Evidence that Hepatic Stellate Cells are Epithelial Progenitors in Adult Mouse Livers. Stem Cells. 2008

29. Russo FP, Alison MR, Bigger BW, Amofah E, Florou A, Amin F, Bou-Gharios G, Jeffery R, Iredale JP, Forbes SJ. The Bone Marrow Functionally Contributes to Liver Fibrosis. Gastroenterology 2006;130:1807–1821. [PubMed: 16697743]

30. Yovchev MI, Grozdanov PN, Zhou H, Racherla H, Guha C, Dabeva MD. Identification of adult hepatic progenitor cells capable of repopulating injured rat liver. Hepatology 2008;47:636–647. [PubMed: 18023068]

NIH-PA Author Manuscript
NIH-PA Author Manuscript
NIH-PA Author Manuscript

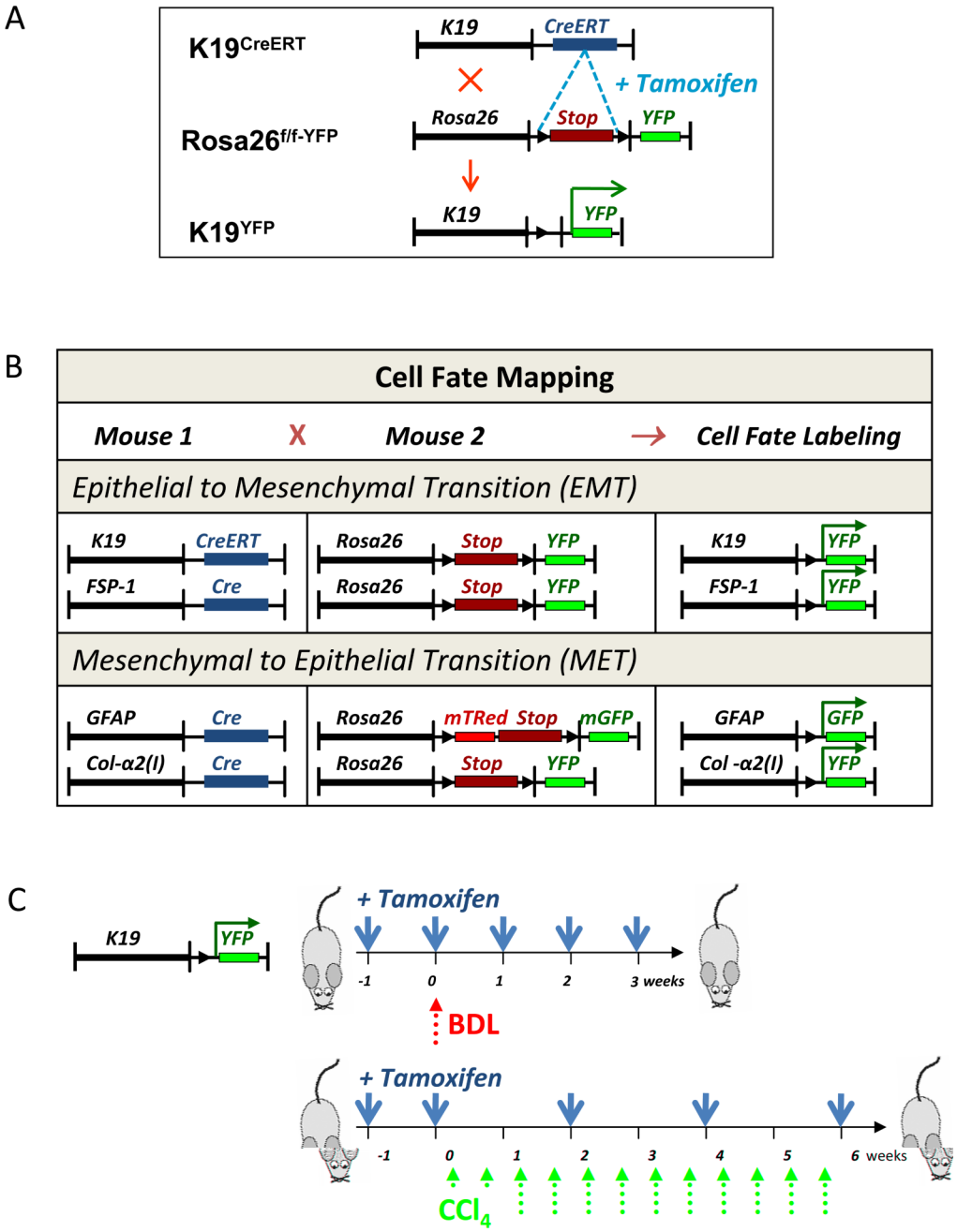

Figure 1. EMT and MET was studied using genetic cell fate mapping in mice in response to liver injury

A) Generation of $K19^{GFP}$ mice to study EMT in $K19^{+}$ cholangiocytes. Upon tamoxifen administration, genetic labeling of cholangiocytes was achieved in $K19^{GFP}$ mice.

B) Summary of genetic crosses in mice. EMT was studied in $K19^{GFP}$ and FSP-1^{YFP} mice. MET was studied in $GFAP^{GFP}$ and $Col2(I)^{YFP}$.

C) Study design: $K19^{YFP}$ mice were treated with tamoxifen (5 mg/mouse) prior and throughout the injury, BDL (3 w) or CCl_4- (0.5 µl/g/corn oil; 6 w). The regimen of tamoxifen administration (blue arrows) and liver injury induction (red arrows) is shown.

NIH-PA Author Manuscript
NIH-PA Author Manuscript
NIH-PA Author Manuscript

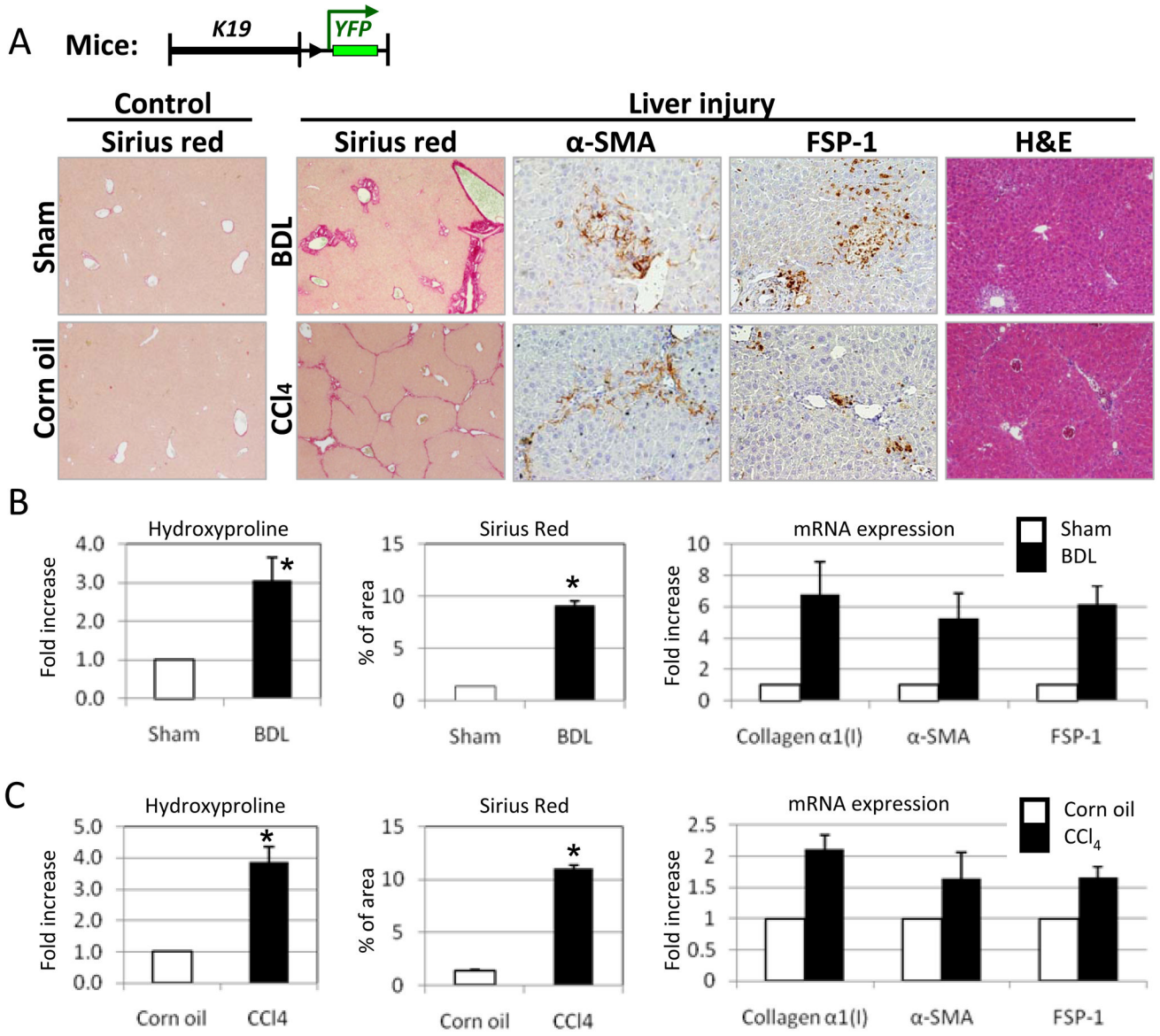

Figure 2. Induction of liver fibrosis in K19^{YFP} mice

A) Liver morphology and fibrosis is assessed K19^{YFP} mice by H&E, Sirius Red staining, immunohistochemistry for α-SMA and FSP-1 expression. Representative images are shown at 20 × and 40 × magnification.

B). Quantification of collagen deposition by hydroxyproline, Sirius red and mRNA expression of collagen α1(I), α-SMA and FSP-1 in response to BDL. (* $p<0.05$, n=10)

C) Collagen deposition and expression of fibrogenic genes were increased in response to CCl_4 treatment (* $p<0.05$, n=10).

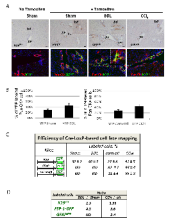

Figure 3. Induction of liver injury in K19^{YFP} mice

A) Tamoxifen-induced Cre-loxP recombination in K19^{Cre} mice, as shown by immunohistochemistry for YFP (upper panel) and immunofluorescence for pancytokeratin (Pan-CK) and YFP (lower panel). Bile ducts (bd), hepatic artery (ha) and portal vein (pv) are indicated.

B) Cre-loxP recombination was quantified in K19^{Cre} mice. The bars display the number of YFP labeled cholangiocytes in comparison with Pan-CK^{+} cholangiocytes (100%) ($p<0,05$, $n=10$).

C) Efficiency of Cre-loxP recombination was estimated in tamoxifen-treated K19^{YFP} mice in comparison with total Pan-CK^{+} cholangiocytes (100%); in GFAP^{GFP} or Col2(I)^{YFP} mice was in isolated myofibroblast fractions (100%) by the number of genetically labeled GFP^{+} or YFP^{+} cells, respectively.

D) Liver injury increases the number of K19^{+}, FSP-1 and GFAP^{+} cells. The number of labeled cells is compared in BDL and sham-operated mice, or in CCl_4- and corn oil-treated mice, and expressed as the ratio calculated for each group.

NIH-PA Author Manuscript NIH-PA Author Manuscript NIH-PA Author Manuscript

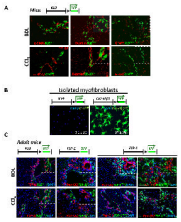

Figure 4. EMT in cholangiocytes does not contribute to the myofibroblast population in response to liver injury

A) In BDL- or CCl_4-injured $K19^{YFP}$ mice, genetically labeled YFP^+ cholangiocytes did not co-express myofibroblast markers (α-SMA, Desmin or GFAP), shown at 400 × magnification.

B) Myofibroblast fraction isolated from BDL-operated $K19^{YFP}$ mice lacked EMT-derived YFP^+ cells, as detected by immonostaining with anti-GFP antibody. As a control, expression of YFP was detected in 97% of plated cells myofibroblasts isolated from CCl_4-treated Col2 $(I)^{YFP}$ mice ($p<0.05$).

C). Liver tissues from $K19^{YFP}$ mice were stained with anti-FSP-1 antibody. Liver sections from FSP-1-GFP reporter mice (n=7) were stained with anti-GFP and anti-Pan-CK antibodies. Similarly, $FSP\text{-}1^{YFP}$ mice (n=8) were stained with anti-GFP and anti-Pan-CK antibodies. Representative images are shown at 40 × and 400 × magnification.

NIH-PA Author Manuscript NIH-PA Author Manuscript NIH-PA Author Manuscript

NIH-PA Author Manuscript
NIH-PA Author Manuscript
NIH-PA Author Manuscript

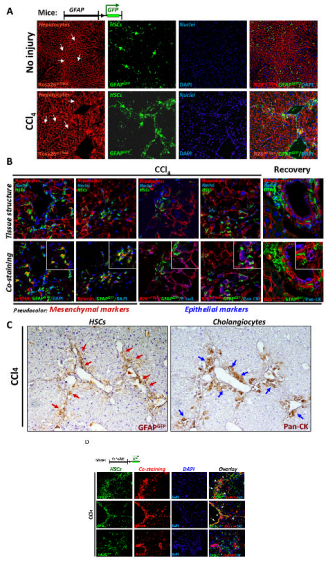

Figure 5. Genetically labeled quiescent or activated HSCs do not undergo MET in response to CCl_4 injury or during recovery

A) Morphology of liver tissues from $GFAP^{GFP}$ mice is shown prior to injury (upper panel) and following CCl_4 administration (lower panel). Quiescent and activated HSCs are labeled by membrane-bound GFP expression (green arrows), and hepatocytes retain expression mTRed (white arrows; 200 × magnification).

B) Genetically labeled $GFAP^{+}$ quiescent HSCs do not express MET markers in response to CCl_4 or during recovery in $GFAP^{Cre}$ mice (n=10). Images show morphology (upper panel) and co-staining (lower panel) of the same tissue section with anti-α-SMA, anti-Desmin, E-cadherin (E-cad) or Pan-CK antibodies and visualized using Alexa-Fluor-633-conjugated secondary antibodies for α-SMA, Desmin (shown in pseudo-red color), and E-cadherin and Pan-CK (pseudo-blue color; 600 × magnification).

C) Serial liver sections from $GFAP^{GFP}$ mice demonstrate differential localization of genetically labeled $GFAP^{+}$ HSCs and Pan-CK^{+} cholangiocytes in response to CCl_4.

D) Genetically labeled activated HSCs do not undergo MET in CCl_4-treated $Col2(1)^{YFP}$ mice (n=10). $Col2(1)^{YFP}$ mice upregulate YFP in all activated HSCs and co-express α-SMA and desmin, but lack Pan-CK expression (200 × magnification).

NIH-PA Author Manuscript

NIH-PA Author Manuscript

NIH-PA Author Manuscript

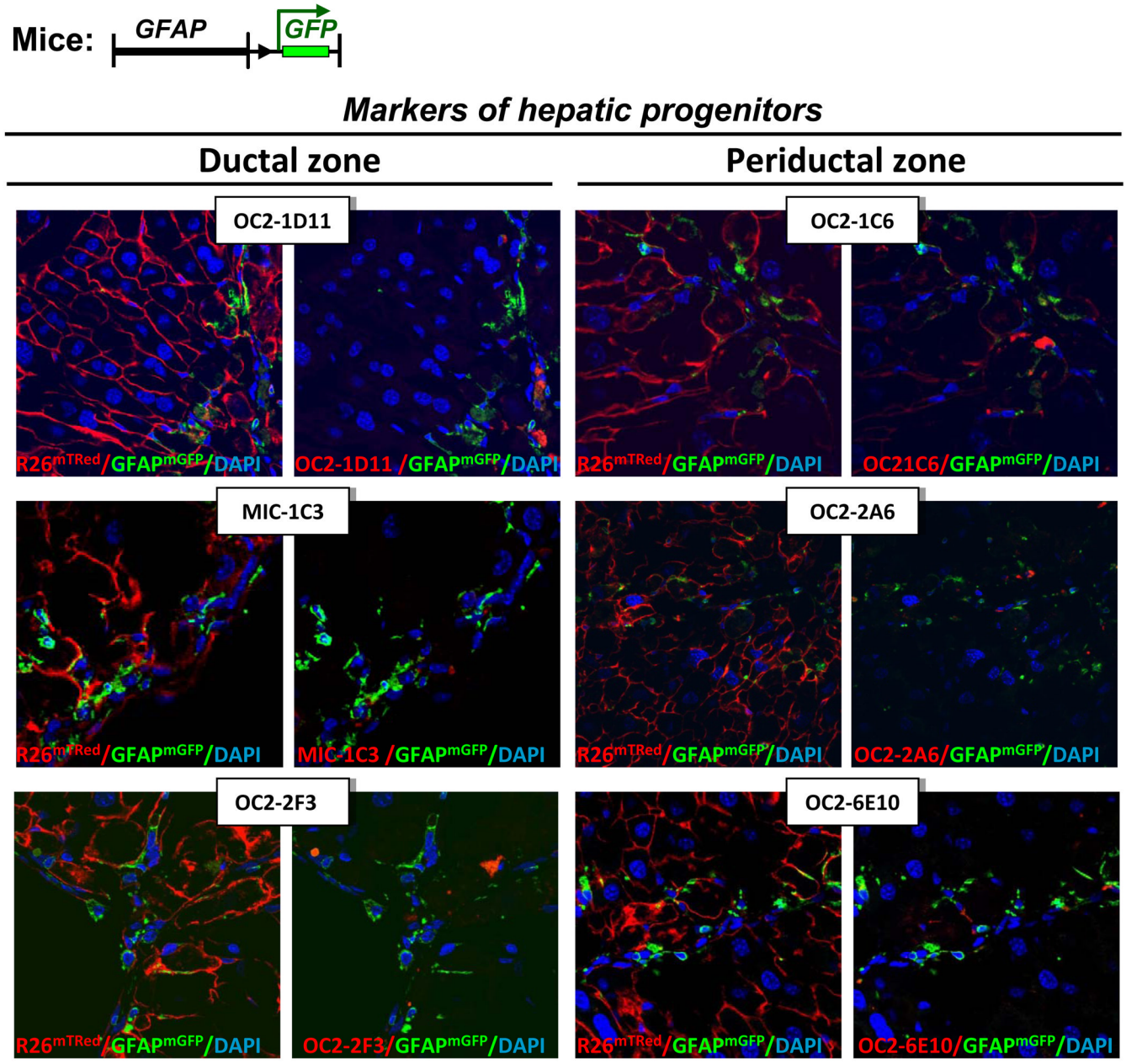

Figure 6. HSCs do not express markers of hepatic progenitor cells in response in CCl_4

Progenitor markers are not co-expressed in $GFAP^{GFP+}$ HSCs. Livers from CCl_4-treated $GFAP^{GFP}$ mice were stained with antibodies that recognize hepatic progenitors in the ductal zone and periductular zone. Tissue structure (left) and co-staining (right) are shown for each immunostaining (pseudo-red color). Representative images are shown at 600 × magnification.

NIH-PA Author Manuscript

NIH-PA Author Manuscript

NIH-PA Author Manuscript

Table 1

The genetic cell fate mapping of transgenic mice used to study EMT and MET: Summary of results

The genetically labeled cell type is stated for each transgenic mouse; co-staining of the cell of interest with other markers is shown, and the presence (++ ; +) or absence (−) of co-expression of specific markers is indicated.

Mouse	Labelling	Co-staining	Co-expression
K19^{YFP}	K19	Pancytokeratin	+
		Troma III	+
		α-SMA	−
		Desmin	−
		FSP-1	−
		GFAP	−
FSP-1^{YFP}	FSP-1	Pancytokeratin	−
GFAP^{GFP}		α-SMA	+
		Desmin	++
		Pancytokeratin	−
		E-cadherin	−
		Oval cell	−
Col2(I)^{YFP}	Collagen α2(I)	E-Cadherin	−
		Pancytokeratin	−
		Desmin	++
Wild type	Pan-CK	α-SMA	−